Depinning of the Bragg Glass in a Point Disordered Model Superconductor

Peter Olsson

Department of Physics, Umeå University, 901 87 Umeå, Sweden

(Received 24 April 2006; revised manuscript received 13 September 2006; published 27 February 2007)

We perform simulations of the three-dimensional frustrated anisotropic XY model with point disorder as a model of a type-II superconductor with quenched point pinning in a magnetic field and a weak applied current. Using resistively shunted junction dynamics, we find a critical current I_c that separates a creep region with immeasurably low voltage from a region with a voltage $V \propto (I - I_c)$ and also identify the mechanism behind this behavior. It also turns out that data at fixed disorder strength may be collapsed by plotting V versus TI, where T is the temperature, though the reason for this behavior as yet not is fully understood.

DOI: 10.1103/PhysRevLett.98.097001 PACS numbers: 74.25.Qt, 74.25.Dw, 74.25.Sv

The behavior of elastic structures in the presence of point disorder is a profound question in condensed matter physics with relevance, e.g., for charge-density waves and vortex lattices and a number of other systems [1]. Already, the static problem is a very difficult one due to the competition between the repulsive interactions, which favor a periodic structure, and both thermal fluctuations and quenched disorder, with the effect to weaken this order. The common picture has for some time been that the quenched disorder turns the vortex lattice into a Bragg glass, which is a phase with algebraically decaying correlations [2,3], though some recent papers suggest a more complicated phase diagram [4,5].

The dynamic properties of a rapidly moving medium in the presence of point disorder is an active field with several open questions and competing scenarios. The present Letter concerns the behavior at weak driving fields. That case has been less discussed, and the usual picture is that of a sharp depinning transition at zero temperature that is rounded through thermal activation at nonzero T.

In this Letter, we present results from dynamic simulations on a three-dimensional (3D) XY model which suggest that the complete picture is more interesting. Whereas we confirm the expected behavior at *low temperatures*, we find a different behavior at higher temperatures with a critical current I_c that separates a creep region with immeasurably low (though nonzero) voltage from a region with a rectilinear behavior. The voltage may furthermore be collapsed in an unexpected way. Our simulations are in many respects similar to Ref. [6], but our longer simulation times make it possible to probe the behavior even at very low drive with higher precision.

The Hamiltonian of the 3D XY model is

$$\mathcal{H}[\theta_i, \Delta_\mu] = -\sum_{\text{bonds}\, i\mu} J_{i\mu} \cos(\theta_i - \theta_{i+\hat{\mu}} - A_{i\mu} - \Delta_\mu / L_\mu). \tag{1}$$

Here, θ_i are the phase angles, the Δ_μ are twist variables [7] in the three Cartesian directions, and the sum is over all links between nearest neighbors. The vector potential $A_{i\mu}$ is chosen such that $\nabla \times A_{i\mu} = 2\pi f \hat{\mathbf{z}}$, and the frustration $f = 1/45$ together with the system size $45 \times 45 \times 32$ gives 45 vortex lines in the system. This low density is important since it reduces the effects of the discretization by the numerical grid. The anisotropy is chosen as $J_{iz}/J = 1/40$, and the disorder is introduced as point defects as in Ref. [8] through a low density ($=1/180$) of plaquettes in the x-y plane with four weak links. The weak links have coupling $(1 - p)J$ instead of J. In this study of the vortex solid, we use disorder strengths up to $p = 0.34$. By measuring the energy of the four links around a vortex at both defect positions and ordinary plaquettes, we find that the pinning energy—the energy needed to displace a vortex from a defect position to an ordinary plaquette—is $E_{\text{pin}} \equiv E_v^0 - E_v^{\text{def}} \approx 4.1p$.

To study the driven vortex solid, we do resistively shunted junction (RSJ) dynamics with fluctuating twist boundary conditions [9], though the twist variable in the z direction is kept fixed, $\Delta_z = 0$. The equations of motion are as in [10], and to integrate them, we use a second order Runge-Kutta method with a dimensionless time step of $\Delta t = 0.1$. The length of each run is typically $(1\text{–}4) \times 10^7 \Delta t$.

In our geometry, the vortex lines extend in the $-z$ direction, and the current is applied along a diagonal, $\hat{\mathbf{u}} = (\hat{\mathbf{x}} + \hat{\mathbf{y}})/\sqrt{2}$. This gives a force f_I along $-\hat{\mathbf{v}} = (\hat{\mathbf{x}} - \hat{\mathbf{y}})/\sqrt{2}$ which is one of the symmetry directions of the vortex lattice. The motion of the vortices gives a change in the twist variable Δ_μ, and the voltage is the time derivative of the twist variable. The voltage per link in the μ direction is given by

$$V_\mu = \frac{1}{L_\mu} \frac{d\Delta_\mu}{dt},$$

and the voltage per link along $\hat{\mathbf{u}}$ becomes $V \equiv V_u = (V_x + V_y)/\sqrt{2}$. We also trace out the vortex lines; the notation $\mathbf{r}_i(z)$ is used for the position in the x-y plane of vortex line i at plane z. The mean-squared fluctuation of the vortex lines $\langle u^2 \rangle$ is also determined. The presented data are for a single

disorder realization, but similar results have also been obtained with other disorder realizations.

In Fig. 1, we show the equilibrium phase diagram obtained from both Monte Carlo (MC) and dynamic simulations. From the MC simulations, we find a solid phase which is separated from the vortex liquid by a first order transition. The boundary between the "Pinned solid" and "Floating solid" regions [11] is from determinations of the linear resistance, which will be discussed elsewhere. (The Floating solid is a finite size effect due to a too small total pinning.) We believe that the Pinned solid phase is a Bragg glass though the difficulty to equilibrate truly large systems has hindered us from studying the expected algebraically decaying correlations [3]. Still, the observed pinning is in accordance with the expected behavior of a Bragg glass with many metastable states separated from one another by large energy barriers. At larger p, there is a sharp vortex glass transition [12,13] though the position of this transition has as yet not been determined for the present model parameters. The solid symbols are the parameter values where the dynamic simulations described below have been performed. The dashed region is where we expect the discrete numerical grid to significantly slow down the dynamics.

We now turn to the dynamic behavior shown by the I-V characteristics. Figure 2 shows such data at $p = 0.32$ and a wide range of temperatures. The inset shows the behavior at low temperatures whereas the main panel displays the rather different behavior at higher T. Note the difference in scale; the inset gives an overview whereas the main panel zooms in on the lower left corner of the inset and gives the behavior at very low currents.

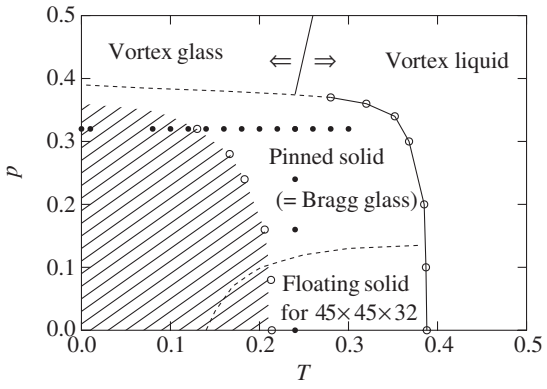

FIG. 1. Equilibrium phase diagram for the simulated model. The open circles connected by a solid line are from determinations of melting temperatures from the vanishing of the structure factor; the continued dashed line is a sketch of a possible behavior at low temperatures. The solid line between "Vortex glass" and "Vortex liquid" indicates the existence of a sharp vortex glass transition [12,13], though—as indicated by the arrows—the precise position has as yet not been determined. The filled circles show the location in the phase diagram of the simulations in Fig. 2 at $p = 0.32$ and the simulations in Fig. 5 at $T = 0.24$. The dashed region is where the numerical grid is expected to significantly affect the dynamics.

As shown in the inset of Fig. 2, there is a sharp transition at $T = 0$ which is significantly rounded already at $T = 0.002$; the data fit nicely to the function $e^{-\text{const}/I}$. This is from a region of the phase diagram where the vortices are strongly pinned by the numerical grid and the energy barrier that governs the dynamics is for a single vortex to move to a neighboring site. To instead examine pinning or depinning from the *disorder*, we turn to higher temperatures and weak currents as shown in the main panel of Fig. 2. The behavior is here very different from the low-T data and suggests the existence of a critical current density I_c which separates the creep region with an immeasurably low voltage at $I < I_c$ from the moving region with $V \propto (I - I_c)$. The relevant barrier is the free energy barrier against displacing the vortex solid one vortex lattice constant $= 5 \times \sqrt{2}(\hat{\mathbf{x}} - \hat{\mathbf{y}})$, from one low energy configuration to another equivalent one. The apparently sharp transition suggests that the relevant energy barrier is much larger than the temperature.

In a further analysis, it was found to be possible to collapse the data by plotting the voltage versus the combination TI, see Fig. 3. We may write $V(T, I) = \chi_V(I/I_c)$ where χ_V is a scaling function and $I_c \propto 1/T$ [14]. In producing the collapse, we discard the data at low T where the dynamics is expected to be strongly affected by the discrete lattice, as discussed further below.

To examine the mechanism behind the temperature dependence of the critical current, we now turn to a simplified model where each of the $L_x L_y L_z f$ sites of a perfect triangular lattice is made into a pinning site with probability 10%. With the pinning distributed in this way, the ground state is a perfect triangular lattice with all pinning sites occupied by vortices. The I-V characteristics in Fig. 4(a) show that this model with $p = 0.08$ also has a critical current which decreases with increasing temperature. To

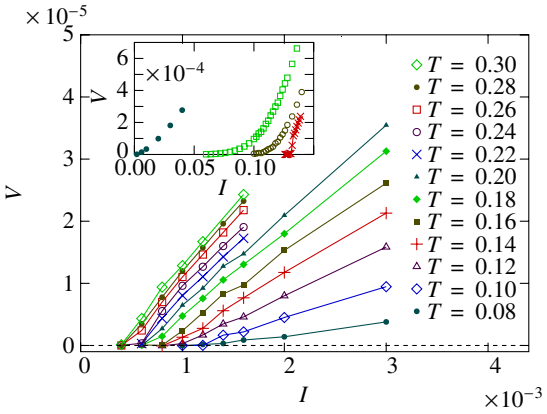

FIG. 2 (color online). I-V characteristics at $p = 0.32$ and several different temperatures. The inset shows the behavior at the temperatures (from right to left), $T = 0.000$, 0.002, 0.010, and 0.080. The main figure shows the behavior at high temperatures and weaker current. The behavior is there strongly affected by the disorder and shows evidence for a sharp change from a creep region to the behavior $V \propto (I - I_c)$ for $I > I_c$.

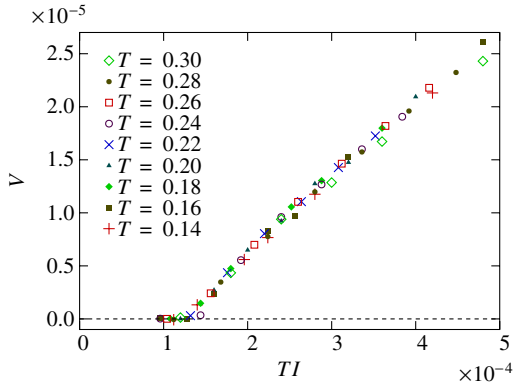

FIG. 3 (color online). Collapse of the I-V characteristics. The voltage at $p = 0.32$ may be collapsed to an impressing accuracy by plotting the data versus TI.

pinpoint the mechanism behind this behavior, we show the fraction of vortices located at pinning sites, ρ_p, for the stationary case, $V \approx 0$, in Fig. 4(b). Focusing first at data with $I = 0$, we find that ρ_p is strongly reduced by increasing T, which clearly is an effect of an increased wandering of the vortex lines. Secondly, ρ_p is reduced by increasing I, and it turns out that the vortex solid only remains immobile for $\rho_p >$ const $\times I$, shown by the dashed line in Fig. 4(b). This means that each pinned vortex can sustain a fixed force (seemingly independent of temperature), but as the current increases and ρ_p/I becomes too small, the vortex solid is set into motion.

The conclusion is now that the increased wandering at higher T or higher I leads to a less efficient pinning, and it seems likely that the same happens in the model with

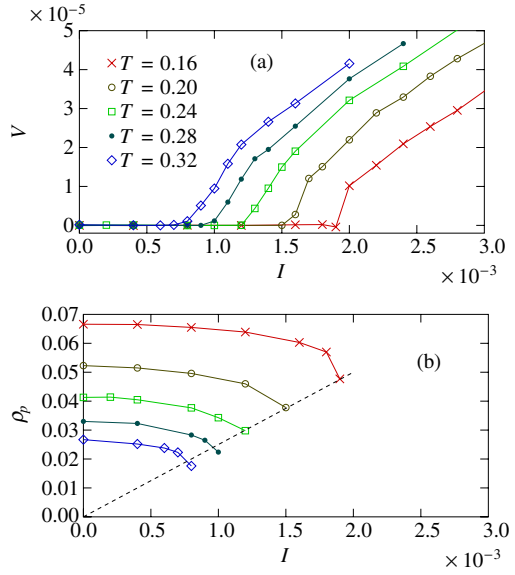

FIG. 4 (color online). Behavior of a simplified system with point pins ordered in a triangular lattice. Panel (a) shows a temperature-dependent onset of the voltage. Panel (b) shows how ρ_p varies with both temperature and current. The vortex solid becomes mobile when ρ_p falls below a certain threshold.

random point pins. A direct verification of this fact in that model is however difficult, since ρ_p is not a good measure of the efficiency of the pinning in that model, as the forces from the randomly distributed pinning sites will point in different directions.

As one more step to improve our understanding of the effect of the disorder, we now examine how the behavior $V = R_0 I$ in the clean system changes with disorder strength. Figure 5 gives the I-V characteristics at constant $T = 0.24$ and four different values of p. The figure shows that a finite p shifts the voltage down towards zero whereas the slope changes only very weakly. This suggests the existence of a force which, much like a friction force, has to be overcome to set the vortices into motion and also reduces the velocity of the moving system.

For a system in equilibrium, one would expect the random pinning to contribute with a number of random

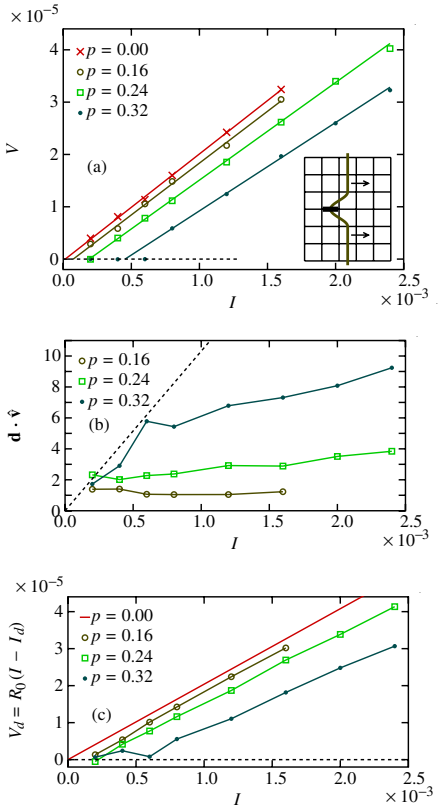

FIG. 5 (color online). Results at $T = 0.24$ and several different p. Panel (a) shows that the effect of a finite p on the I-V characteristics is to shift the data down towards zero. This gives a creep region with very low voltage at low currents, $I < I_c$, and a region with a rectilinear behavior at larger I. The inset illustrates the suggested mechanism: when a vortex line moves in the direction of the applied force, the vortices at defect positions will on the average lag behind the moving vortex lattice. Panel (b) gives the displacement, c.f. Eq. (2) in the direction opposite to f_I. Panel (c) is a calculation of the voltage from R_0 of the pure system and I_d from the measured d and Eq. (3), which shows that the suggested mechanism captures the essential elements of the dynamics.

forces which cancel one another out, but the slow drift of the vortices opens up for other possibilities. We propose a mechanism where some of the vortices at the pinning centers lag behind the unpinned vortices. This leads to a distortion of the elastic vortex lines (see inset of Fig. 5(a)), and also a force f_d from the defect vortices on the vortex lattice. The motion would then be in response to the total force $f_I - f_d$, which is in good agreement with the behavior in Fig. 5(a).

To try to put this on a more solid footing, we introduce a defect operator $D(\mathbf{r}, z)$ which is unity at a defect and zero otherwise. The average position of all nondefect vortices belonging to the same vortex line is then,

$$\bar{\mathbf{r}}_i = \overline{[1 - D(\mathbf{r}_i(z), z)]\mathbf{r}_i(z)}.$$

As a measure of the lagging behind of the defect vortices, we introduce the displacement $\mathbf{d}$, as the sum of their deviations from the average vortex line positions,

$$\mathbf{d} = \left\langle \sum_i \sum_z (\mathbf{r}_i(z) - \bar{\mathbf{r}}_i) D(\mathbf{r}_i(z), z) \right\rangle. \quad (2)$$

Figure 5(b) is a confirmation on a qualitative level of this idea. With the motion along $-\hat{\mathbf{v}}$, the positive value of $\mathbf{d} \cdot \hat{\mathbf{v}}$ shows that the defect vortices on the average lag somewhat behind the ordinary vortices. (We remark that this estimate of the displacement only contains contributions relative to the vortex lines whereas the total displacement also should include effects due to a vortex line or a set of vortex lines lagging behind the rest of the vortex lattice. This is however considerably more difficult to estimate, and as we will see, it seems that the expression above contains the dominant contribution.)

For a quantitative check one would like to compare the magnitude of this defect force f_d with f_I from the applied current. We do a similar comparison by instead estimating I_d, the current density in the system due to the displaced vortices. Recall that the creation of a vortex pair in a 2D model with a separation of d lattice constants in the y direction creates d rows in the x direction where the phase angle rotates by 2π. This gives a total current $I_{\text{tot}} \approx d \sin(2\pi/L_x) \approx 2\pi d/L_x$. Taking this over to our 3D system, we conclude that a displacement d corresponds to a current density

$$I_d = \frac{I_{\text{tot}}}{L_y L_z} \approx \frac{2\pi}{\mathcal{V}} d, \quad (3)$$

and the measured $\mathbf{d} \cdot \hat{\mathbf{v}}$ together with R_0 from the pure system gives an estimate of the voltage, $V_d = R_0(I - I_d)$. Figure 5(c) shows that this V_d (obtained from $\mathbf{d}$) is in good agreement with the measured voltage shown in Fig. 5(a), and this suggests that our simple description in terms of the lagging behind of the defect vortices indeed captures the essential elements of the dynamics.

To obtain the collapse in Fig. 2, it was necessary to discard the points at low temperatures. The rationale was that the discretization of the system at low temperatures reduces the voltage, and the criterion for large effects of the discretization was $\langle u^2 \rangle \lesssim 1$. This criterion is adopted from the behavior in a clean system of the linear resistance, R_l, which is proportional to the diffusion constant for the vortex line lattice. At temperatures below $T \approx 0.14$, the vortex lattice is pinned to the numerical grid, $R_l = 0$. R_l then increases rapidly with increasing temperature up to $T \approx 0.22$ where the increase becomes much slower. From this, we conclude that the effect of the numerical grid to slow down the dynamics is significant at $T \lesssim 0.22$. At $T = 0.22$, the mean-squared fluctuation of the vortex lines is $\langle u^2 \rangle = 1.03$, which leads to our criterion $\langle u^2 \rangle < 1$ for significant effects of the numerical grid. This is the dashed region in Fig. 1.

To conclude, we have examined how point disorder affects the I-V characteristics of a frustrated 3D XY model and have found an unexpected behavior with a critical current that separates the creep region at $I < I_c$ from a region with $V \propto (I - I_c)$. Whereas it was possible to understand the behavior at a qualitative level, the reason for the collapse when plotting the data versus TI remains enigmatic and calls for further investigations.

We acknowledge discussions with S. Teitel and P. Minnhagen, support by the Swedish Research Council through Contract No. 2002-3975, and access to the resources of the Swedish High Performance Computing Center North (No. HPC2N).

[1] A. M. Ettouhami and L. Radzihovsky, Phys. Rev. B **67**, 115412 (2003).
[2] T. Nattermann, Phys. Rev. Lett. **64**, 2454 (1990).
[3] T. Giamarchi and P. Le Doussal, Phys. Rev. Lett. **72**, 1530 (1994).
[4] H. Beidenkopf, N. Avraham, Y. Myasoedov, H. Shtrikman, E. Zeldov, B. Rosenstein, E. H. Brandt, and T. Tamegai, Phys. Rev. Lett. **95**, 257004 (2005).
[5] D. Li and B. Rosenstein, Phys. Rev. Lett. **90**, 167004 (2003).
[6] A. D. Hernández and D. Domínguez, Phys. Rev. Lett. **92**, 117002 (2004).
[7] P. Olsson, Phys. Rev. Lett. **73**, 3339 (1994).
[8] Y. Nonomura and X. Hu, Phys. Rev. Lett. **86**, 5140 (2001).
[9] B. J. Kim, P. Minnhagen, and P. Olsson, Phys. Rev. B **59**, 11506 (1999).
[10] Q.-H. Chen and X. Hu, Phys. Rev. Lett. **90**, 117005 (2003).
[11] A horizontal phase boundary was also found in a different phase diagram in Fig. 4 of [10]. It is unclear if there is any real connection or if this is just a superficial similarity.
[12] P. Olsson, Phys. Rev. Lett. **91**, 077002 (2003).
[13] P. Olsson, Phys. Rev. B **72**, 144525 (2005).
[14] Some additional simulations where the disorder was introduced by random couplings as in Ref. [15] with $p = 0.08$, gave a similar collapse. This is evidence that the obtained behavior is a general one, independent of details of the system.
[15] P. Olsson and S. Teitel, Phys. Rev. Lett. **87**, 137001 (2001).